Variability of the Gyroid Structure for Biomedical Applications

A. Jíra[1,*], L. Řehounek[1], G. Javorská[1]

[1] *Czech Technical University in Prague, Faculty of Civil Engineering, Thákurova 7, 166 29 Prague 6, Czech Republic*

[*] *jira@fsv.cvut.cz*

Abstract: This work deals with gyroid structures and their high level of variability. By manipulating the basic gyroid equation, we can create various structures with either tubular or sheet character. Various specimens created by additive manufacturing are subsequently mechanically tested with the goal of comparing the effectiveness of individual geometrical solutions. The tests showed that gyroid structures offer much greater values of mechanical properties despite having the same porosity as other porous structures. Detailed tests of basic element cells also showed the importance of maintaining periodicity for conservation of isotropic properties of the basic element cell. Isotropy of the basic element cell is an important characteristic for subsequent numerical analyses utilizing the numerical homogenisation method.

Keywords: gyroid; 3D printing; osseointegration surface; gyroid variations.

1 Introduction

An optimal porous surface is the basis of every implant [1]. With the advancement of additive technologies, it is now possible to manufacture structures varying between the trabecular and sheet-based geometry [2, 3]. While a thicker porous structure in big implants does not pose a problem for greater trabecular beams, small implants only lend themselves to small diameters of beams and it is not uncommon to reach the lower precision limit of the machine, which poses quality risks [4]. A viable alternative is the gyroid structure. The gyroid structure is described by Eq. (1) and enables for a wide variety of the final shape and overall behavior.

$$F(x,y,z) = F_{sg}(x,y,z) = t = \sin(\bar{x}) \cdot \cos(\bar{y}) + \sin(\bar{y}) \cdot \cos(\bar{z}) + \sin(\bar{z}) \cdot \cos(\bar{x}), \tag{1}$$

where $\bar{x}$, $\bar{y}$ a $\bar{z}$ are modified spatial coordinates so that $\bar{x} = 2\pi x/a$, $\bar{y} = 2\pi y/a$ a $\bar{z} = 2\pi z/a$. And parameter t determines the boundary curvature of the whole structure and therefore its overall character. A gyroid structure specified this way is called the Single gyroid ($F = F_{sg}$) and its applicability is very wide [5, 6].

Fig. 1 shows variants of the gyroid structure with different values of the parameter t. From this comparison, we can see that by roughly defining $t \in \langle 0.6; 1.2)$ and $t \in (-1.2; -0.6\rangle$, a tubular structure resembling beams is created. On the contrary, if we define $t \in (-0.6; 0.6)$, a sheet structure is created. The gyroid structure is defined for $-1.5 < t < 1.5$. If we set the parameter t between $1.2 < |t| < 1.5$ the structure will be defined, but various discontinuities and defects in continuity and smoothness can emerge [7].

The gyroid structure can be defined by two single gyroids with opposite orientations of surface curvature – the double gyroid. The structure is, therefore, represented twice and its volume is greater as compared to the single gyroid [5]. The basic equation for the double gyroid $F = F_{dg}$ can be written as following:

$$F(x,y,z) = F_{dg}(x,y,z) = t^2 = \big(\sin(\bar{x}) \cdot \cos(\bar{y}) + \sin(\bar{y}) \cdot \cos(\bar{z}) + \sin(\bar{z}) \cdot \cos(\bar{x})\big)^2, \tag{2}$$

where t is a parameter influencing the surface curvature and is defined in the range of $t \in \langle -1.413; 1.413\rangle$ for the double gyroid.

2 Methodology

The influence of parameter t on the gyroid geometry is shown on Fig. 2. By defining $t \in \langle 0; 0.4\rangle$, two sheet gyroids are created. When intersected with a homogeneous volume, a gyroid structure with a defined wall thickness is created. This is the second way of creating a volume. Parameter $t \in \langle 0.6; 1.2\rangle$ creates a vastly more dense tubular structure than the single gyroid variant shown on Fig. 1.

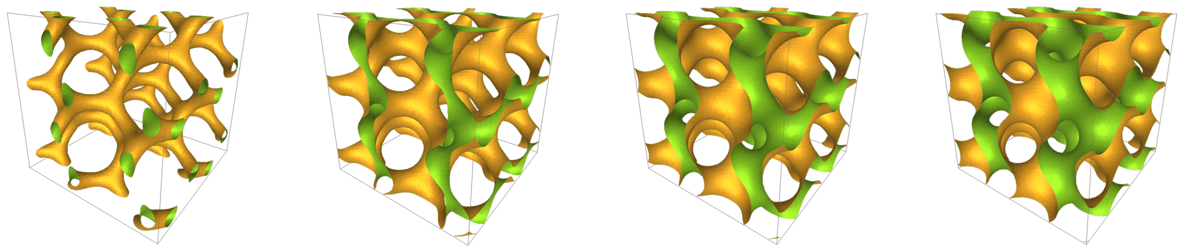

(a) $t = -1.2$ (b) $t = -0.9$ (c) $t = -0.6$ (d) $t = -0.3$

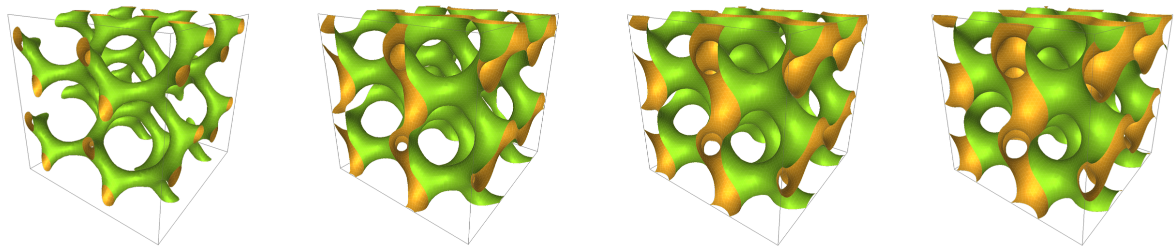

(e) $t = 1.2$ (f) $t = 0.9$ (g) $t = 0.6$ (h) $t = 0.3$

Fig. 1: Variants of the gyroid structure modelled according to Eq. (1) with different values of parameter t.

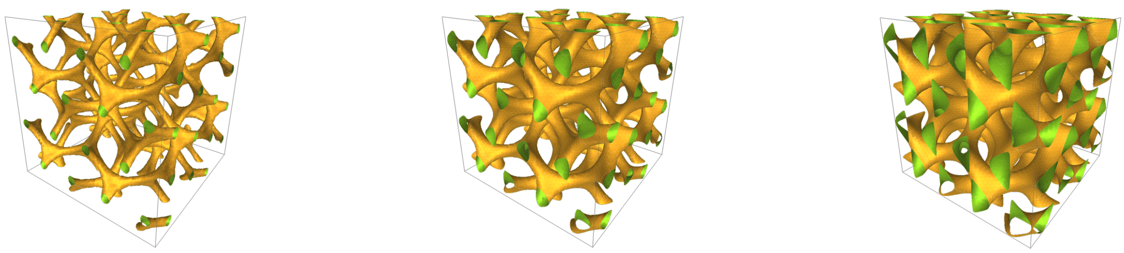

(a) $t = 1.2$ (b) $t = 1.0$ (c) $t = 0.8$

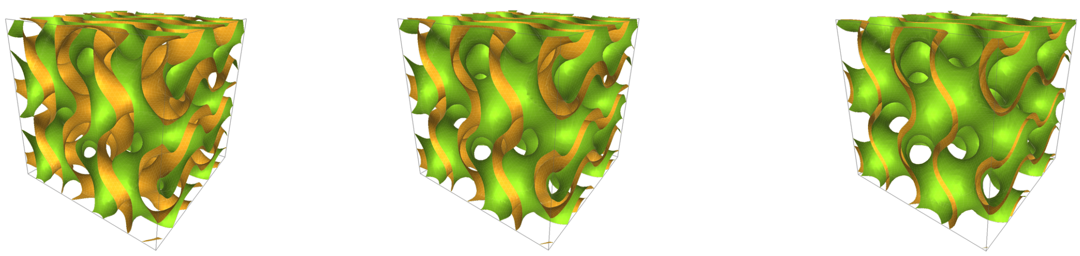

(d) $t = 0.3$ (e) $t = 0.4$ (f) $t = 0.2$

Fig. 2: Variants of the double gyroid structure modelled according to Eq. (2) with different values of parameter t.

Structures shown on Fig. 1 and 2 were generated in the MathMod software, version 11 [8] and the figures show a structure in a circumscribed cube of 2.5π edge length for demonstration purposes of periodically composed cells. The great variability of the structure gives rise to a question – how will these two variants (tubular and sheet) of the structure behave in comparison? This question can be answered by experiment.

The gyroid structure, which is defined by an implicit equation (Eq. (1)) enables for shaping of the structural character (tubular v. sheet) and influences porosity, an important characteristic for osseointegration of implants in bone cavities. [9].

The specimens were designed in Autodesk NetFabb and 3D-printed on the SLS Sinterit Lisa Pro printer. The dimensions of the porous parts were $25.12 \times 25.12 \times 25.12$ mm and a 2 mm thick load-distributing homogeneous plate was added on the top and bottom ends (Fig. 3). The porous part consisted of 4^3 cells with individual dimensions of $6.28 \times 6.28 \times 6.28$ mm. The porous structure is derived from Eq. (1) for the single gyroid. The sheet variant corresponds to a structure with $t = 0$ and explicitly defined wall thickness of 0.5 mm. The tubular version of the gyroid corresponds to parameter $t = 0.78$. Both variants modelled this way have the same porosity of $n = 0.75$.

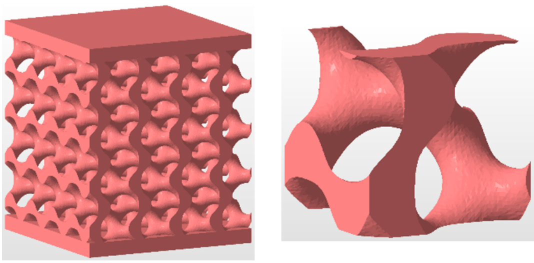

(a) tubular gyroid

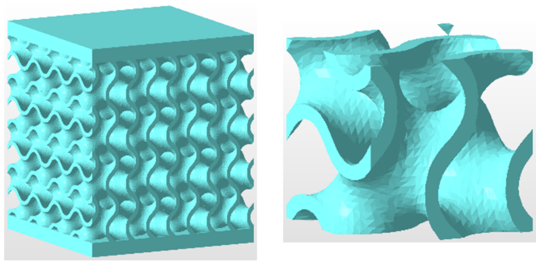

(b) sheet gyroid

Fig. 3: Geometrical models of test specimens and basic element cells – (a) tubular gyroid, (b) sheet gyroid [7].

Specimens shown on Fig. 3 were 3D-printed out of polyamide (PA12) and subsequently loaded on the LiTeM machine in the mode of controlled displacement with speed of 0.04 mm/s until failure.

3 Results and conclusion

The graphs on Fig. 4 show a significant difference in ultimate force and elastic modulus. The sheet variant of the gyroid structure reached an ultimate compressive strength of 4.43 ± 0.47 MPa, while the tubular variant reached only 1.75 ± 0.11 MPa. Similar differences can be observed in numerical analyses of the global modulus of the porous structure E, which was $E = 72.43 \pm 6.13$ MPa for the sheet variant, while only $E = 28.74 \pm 1.80$ MPa for the tubular variant. Therefore, the sheet variant reaches much better values of mechanical parameters at the same level of porosity and presents a more advantageous solution for load-bearing parts of implants.

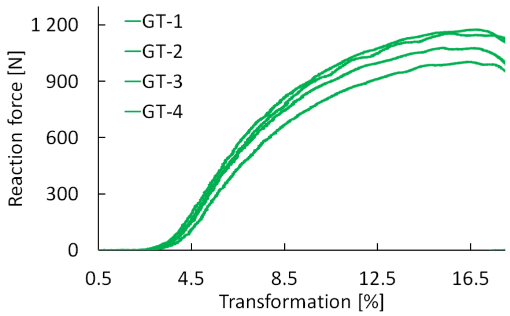

(a) tubular gyroid

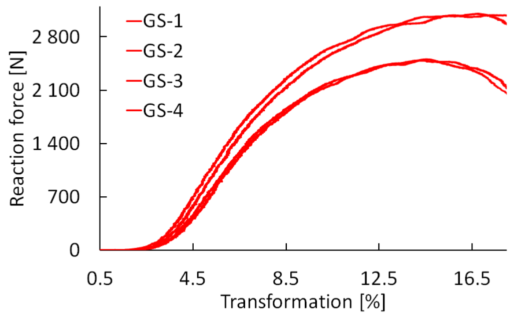

(b) sheet gyroid

Fig. 4: Force-displacement diagrams of tested structures manufactured via 3D printing from the PA12 material. (a) – tubular gyroid (GT), (b) – sheet gyroid (GS).

On Fig. 5, we can see sequential shots from the mechanical tests with differences in deformations of individual specimens. The choices of images on Fig. 5 are, beginning from left: test start, halfway through the test and at the end, following failure. The images show greater that the sheet gyroid structure has greater strength and stiffness as compared to the tubular variant. Both structures show formation of crack leading to total failure of the specimens. Different values of ultimate stress are shown on graphs on Fig. 4. They confirm the fact that the sheet variant of the organic structure is a viable alternative in regard to its greater strength.

In spite of being a TPMS (Triply Periodic Minimal Surface), the gyroid's periodicity can vary and depends on the section made in the structure. Periodicity is important for subsequent numerical analyses via FEM utiliz-

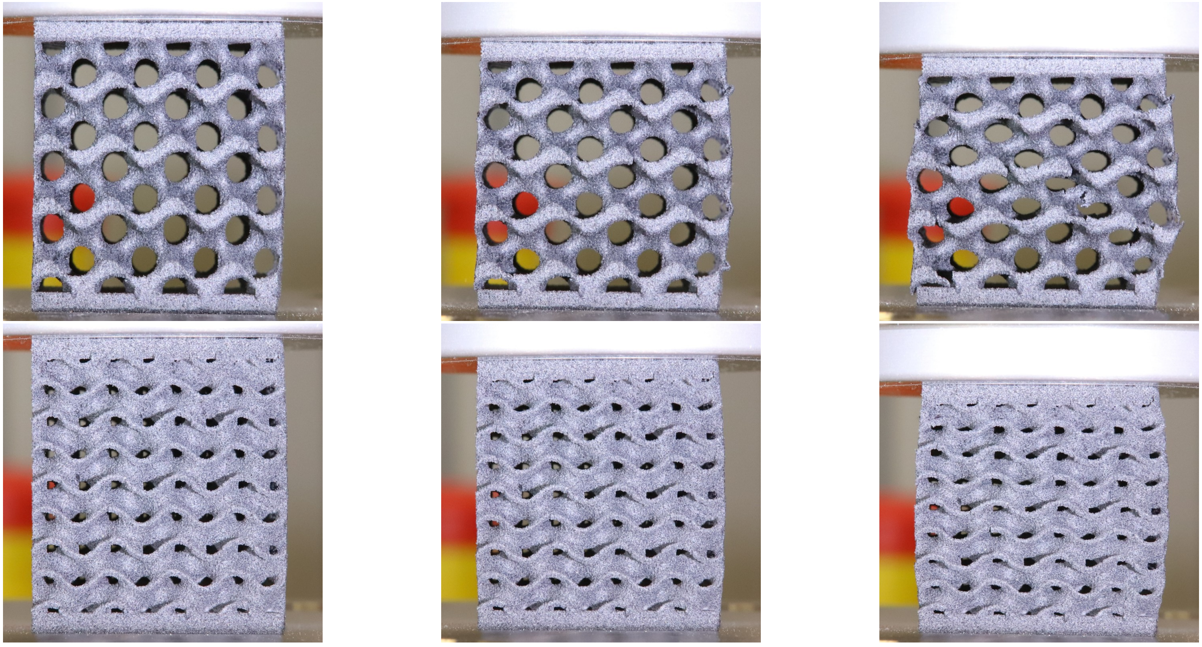

Fig. 5: Example of specimens deformation during the uniaxial compression test. Top row is the tubular gyroid variant, bottom row is the sheet gyroid.

Tab. 1: Parameters of the basic gyroid element cell for verification of symmetry and isotropy.

	cell dimensions [mm]	wall thickness [mm]	cell period in axial direction x	y	z
sample 1	$12,56 \times 12,56 \times 12,56$	0,5	$-\pi; +\pi$	$-\pi; +\pi$	$-\pi; +\pi$
sample 2	$12,56 \times 12,56 \times 12,56$	0,5	$-\pi; +\pi$	$-\frac{1}{2}\pi; +\frac{3}{2}\pi$	$-\pi; +\pi$

ing the numerical homogenisation method. For verifying the influence of periodicity on mechanical properties of the basic element cell, another static mechanical test was performed, using the same parameters as the former experiment. Specimens containing only one cell of the sheet single gyroid were made using 3D printing from the PA12 material (Tab. 1).

A simple comparison based on the mechanical tests of a single cell showed that a cell with the same period in all axes is isotropic. On the contrary, if we change the period by $\pi/2$ in the direction of one axis, the behavior changes to ortotropic (Fig. 6). With a specimen comprised of multiple periodical cells, we predict this influence of period offset will be eliminated and the overall response will be isotropic. However, for the purposes of using the gyroid cell for homogenisation and numerical FEM analyses, it is necessary to use a basic element cell that has the same period in all three axes.

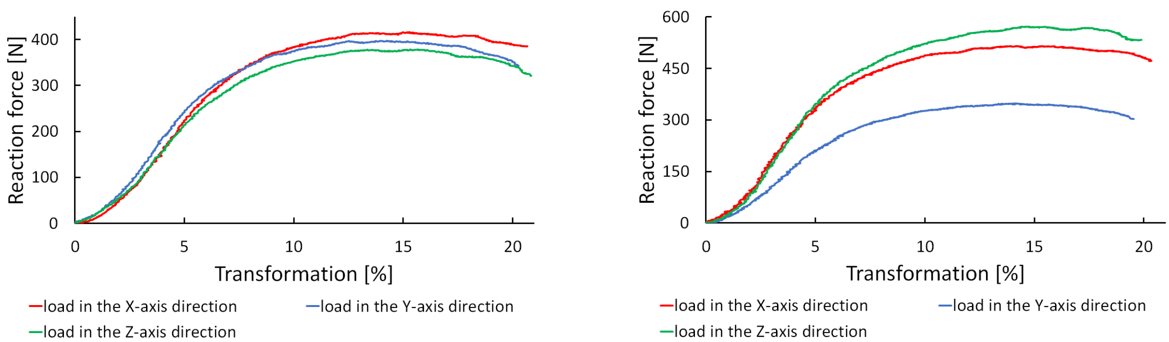

Fig. 6: A comparison of mechanical behavior of a single gyroid cell with the same period in all axes (a) and a gyroid cell with a period offset by $\pi/2$ in the direction of the y axis (b)

Acknowledgement

This work was carried out with the financial support of an internal CTU grant n. SGS 161 1612078A132.

References

[1] L. Řehounek, F. Denk and A. Jíra, Geometrical optimization of dental implants with regard to osseointegration, Acta Polytechnica CTU Proceeding 13 (2017) 97–101, doi: 10.14311/APP.2017.13.0097.

[2] P. Szymczyk, et al., The effect of geometry on mechanical properties of Ti6Al4V ELI scaffolds manufactured using additive manufacturing technology, Archives of Civil and Mechanical Engineering 20 (2020) 1–13, doi: 10.1007/s43452-020-0011-y.

[3] E. Gawronska and R. Dyja, Numerical Study of Geometry's Impact on the Thermal and Mechanical Properties of Periodic Surface Structures, Materials 14 (2021) 1–14, doi: doi.org/10.3390/ma14020427.

[4] A. Jíra, P. Hájková and L. Řehounek, Trabecular structures as efficient surface of dental implants, 57th International Scientific Conference on Experimental Stress Analysis, Luhačovice, Czech Republic (2019) 169–174.

[5] E. Yang, et al., Effect of geometry on the mechanical properties of Ti-6Al-4V Gyroid structures fabricated via SLM: A numerical study, Material and Design 184 (2019) 1–24, doi: 10.1016/j.matdes.2019.108165.

[6] M. Niinomi, Mechanical properties of biomedical titanium alloys, Materials Science and Engineering, 234 (1998) 231–236, doi: 10.1016/S0921-5093(97)00806-X.

[7] A. Jíra, et al,. Mechanical Properties of Porous Structures for Dental Implants: Experimental Study and Computational Homogenization, Materials 14 (2021) 1–25, doi: 10.3390/ma14164592.

[8] A. Taha, MathMod open source (GPL), Retrieved from: https://sourceforge.net/projects/mathmod/.

[9] M. Geetha, et al., Ti based biomaterials, the ultimate choice for orthopaedicimplants – A review, Progress in Materials Science, 54 (2009) 397–425, doi: 10.1016/j.pmatsci.2008.06.004.